


Exploration of *Wedelia chinensis* leaf-assisted silver nanoparticles for antioxidant, antibacterial and in vitro cytotoxic applications

Follow this and additional works at: <https://www.jfda-online.com/journal>

 Part of the [Food Science Commons](#), [Medicinal Chemistry and Pharmaceutics Commons](#), [Pharmacology Commons](#), and the [Toxicology Commons](#)



This work is licensed under a [Creative Commons Attribution-Noncommercial-No Derivative Works 4.0 License](#).

Recommended Citation

Paul, Das M.; Rebecca, Livingstone J.; Veluswamy, P.; and Das, J. (2018) "Exploration of *Wedelia chinensis* leaf-assisted silver nanoparticles for antioxidant, antibacterial and in vitro cytotoxic applications," *Journal of Food and Drug Analysis*: Vol. 26 : Iss. 2 , Article 41.

Available at: <https://doi.org/10.1016/j.jfda.2017.07.014>

This Original Article is brought to you for free and open access by Journal of Food and Drug Analysis. It has been accepted for inclusion in Journal of Food and Drug Analysis by an authorized editor of Journal of Food and Drug Analysis.

Available online at www.sciencedirect.com

ScienceDirect

journal homepage: www.jfda-online.com

Original Article

Exploration of *Wedelia chinensis* leaf-assisted silver nanoparticles for antioxidant, antibacterial and in vitro cytotoxic applications



Merina Paul Das ^{a,*}, Jeyanthi Rebecca Livingstone ^a,
Pandiyarasan Veluswamy ^b, Jayabrata Das ^c

^a Department of Industrial Biotechnology, Bharath University, Chennai 600 073, Tamil Nadu, India

^b Department of Electronics and Material Science, Research Institute of Electronics, Shizuoka University, Hamamatsu 432-8011, Japan

^c Department of Biotechnology, School of Bioengineering, SRM University, Kattankulathur, Chennai 603 203, Tamil Nadu, India

ARTICLE INFO

Article history:

Received 24 April 2017

Received in revised form

5 July 2017

Accepted 7 July 2017

Available online 31 August 2017

Keywords:

Wedelia chinensis

AgNPs

Antioxidant

Antibacterial

Cytotoxicity

ABSTRACT

Green synthetic route of silver nanoparticles (AgNPs) has already been proved to be an advantageous over other physico-chemical approaches due to its simplicity, cost effectiveness, ecofriendly and nontoxicity. In this finding, aqueous *Wedelia chinensis* leaf extract (WLE) mediated synthesis of AgNPs was approached. Surface plasmon resonance (SPR) band at 408 nm preliminary indicated the formation of AgNPs, while TEM and XRD characterization confirmed the formation of spherically shaped and crystalline AgNPs with an average size of 31.68 nm, respectively. The plausible biomolecules in the aqueous leaf extract responsible for the reduction and stabilization of AgNPs were identified by FTIR analysis and found to be polyphenolic groups in flavonoid. Further, synthesized AgNPs was explored for different biological applications. Biosynthesized AgNPs showed significant free radical scavenging activity as compared to *Wedelia* leaf extract and antibacterial activity against clinically isolated test pathogens where Gram-negative bacteria were found more susceptible to AgNPs than Gram-positive one. In addition, in vitro cytotoxic response was also evaluated on hepatocellular carcinoma Hep G2 cell lines and showed a dose-dependent cytotoxic response with an IC₅₀ value of 25 µg/mL.

Copyright © 2017, Food and Drug Administration, Taiwan. Published by Elsevier Taiwan LLC. This is an open access article under the CC BY-NC-ND license (<http://creativecommons.org/licenses/by-nc-nd/4.0/>).

* Corresponding author.

E-mail address: merinadas@gmail.com (M. Paul Das).

<http://dx.doi.org/10.1016/j.jfda.2017.07.014>

1021-9498/Copyright © 2017, Food and Drug Administration, Taiwan. Published by Elsevier Taiwan LLC. This is an open access article under the CC BY-NC-ND license (<http://creativecommons.org/licenses/by-nc-nd/4.0/>).

1. Introduction

This era has witnessed the inception of novel technological products specifically based on nanotechnology, and nanomaterial synthesis is being widely explored since they exhibit distinctive size and shape dependent properties in various applications like catalytic systems, optoelectronics, biomedical etc. [1–4]. Huge varieties of nanomaterials are engineered to be introduced directly into the body for the therapeutic and diagnostic purpose [5]. It has been proved over the years that size of the nanoparticle is important to improve their biocompatibility as well as bioavailability for therapeutical applications in diseases like cancer [6]. Among the nanoparticles, silver nanoparticles (AgNPs) play a significant role in the cancer management by preventing the ATP synthesis in mitochondria and altering the essential metabolic pathways for cell survival [7,8]. According to Food and Drug Administration (FDA) report, AgNPs are particularly found to be effective against microbial mediated diseases and possess an immense potential in treating diseases like AIDS, cancer, retinal neovascularization, hepatitis B, diabetes, etc. in the near future [9].

The oxidation reaction is crucial for the production of cellular energy, but consequently generates a large amount of oxygen-derived free radicals as by-products and initiate chain reaction. Resulting damage of various complex biomolecules like protein, lipid, carbohydrate, DNA which ultimately associated with many health issues related to heart diseases, cancer, aging, renal failure etc. [10,11]. Antioxidants play an essential role in preventing the oxidative stress by terminating the chain reaction. AgNPs have been reported to be an effective free radical scavenger due to donating properties of an electron or hydrogen to a oxidant to form a stable molecule [12,13]. Apart from antimicrobial and cytotoxic responses, antioxidant studies also have prime importance and researches are still underway to clarify these aspects.

Recent days several attempts have been made to fabricate AgNPs with controlled size and shapes [14]. However, most of the wet chemical methods reported rely heavily on organic solvents and use hazardous reducing agents [15]. Hence, there is an increased interest to design a green chemistry route to minimize or eliminate the use and generation of toxic substances in synthetic processes [16]. Even though a number of plants have already been attempted to synthesize AgNPs, but synthesizing nanoparticles with controlled size and various morphologies are still great challenges. Initially, Gardea-Torresdey et al. identified the plant as a potential biomaterial to synthesize metal nanoparticles [17]. Later on, one pot biosynthesis of stable nanomaterials with different dimensions was extensively studied for industrial needs [18,19].

To date no reports have been documented on biogenic synthesis of AgNPs using the abundantly and commercially available *Wedelia chinensis* as a biomaterial. The plant has been claimed to have significant therapeutics effects in the management of cancer, inflammation, wound healing, CNS disorder, ulcer, etc. *Wedelia* also known for its antioxidant and antimicrobial activities due to the presence of active constituents such as triterpenoids, flavonoids, and wedelolactones, and the research is still in progress to find uses for them [20].

Hence, the present research was aimed to investigate the synthesis and characterization of the AgNPs and to explore for antioxidant, antibacterial and *in vitro* cytotoxic properties.

2. Materials and methods

2.1. Chemicals

Silver nitrate (AgNO_3), fetal bovine serum (FBS), Dulbecco's modified eagle medium (DMEM), phosphate buffer solution (PBS), dimethyl sulfoxide (DMSO), methyl thiozolyldiphenyl-tetrazolium bromide (MTT), potassium ferricyanide ($\text{K}_3\text{Fe}(\text{CN})_6$), L-ascorbic acid (AA), 2,2-diphenyl-1-picrylhydrazyl (DPPH), trichloroacetic acid (TCA), ferric chloride (FeCl_3) were obtained from Sigma Chemicals, India and used as such without any further purification.

2.2. Biosynthesis of AgNPs

Freshly collected *W. chinensis* leaves were thoroughly washed, shade dried and powdered for experimental use. To prepare *Wedelia* leaf extract, 10 g of leaf powder in 100 mL Milli Q water was heated to boil for 15 min and centrifuged to collect the leaf extract. To carry out the biosynthesis, varying amounts (0.1–1.0 mL or 1–10% v/v) of leaf extract were separately added to 9 mL of 1 mM AgNO_3 solution. The final volume of the reaction mixture was kept constant to 10 mL by adding Milli Q water and heated at 60 °C until yellowish brown color appears. UV–vis spectra were then observed to confirm the formation of AgNPs. Finally, the synthesized AgNPs in solution were purified by repeated centrifugation at 10,000 rpm for 10 min and dried using lyophilizer.

2.3. Characterization of biosynthesized AgNPs

Surface plasmon resonance (SPR) spectra of thus synthesized AgNPs were confirmed using UV–visible double spectrometer (Perkin–Elmer spectrophotometer) within the range of 300–700 nm. The morphology and elemental composition of the AgNPs were characterized using transmission electron microscopy (TEM; JEOL-2010), energy-dispersive X-ray spectroscopy (EDX; Sigma), X-ray diffraction (XRD; X'Pert Pro A Analytical), X-ray photoelectron spectroscopy (XPS; ESCALAB 210) analysis. To identify the possible biomolecules associated in the synthetic process, FTIR (Cary 600 Agilent) of *Wedelia* leaf extract was performed before and after addition to the AgNO_3 solution.

2.4. Antioxidant assays

Antioxidant activity of the biosynthesized AgNPs were evaluated using two different methods as follows, where *Wedelia* leaf extract and L-ascorbic acid (AA) were considered as a control and reference, respectively.

2.4.1. DPPH free radical scavenging assay

The DPPH free radical scavenging activity of biosynthesized AgNPs was carried out as described by Chang et al. [21]. Briefly, different concentrations of AgNPs (12.25, 25, 50, 100, and

200 µg/mL) in methanol were mixed separately with equal volume of 0.3 mM of DPPH and incubated at room temperature for 30 min. Absorbance (A) of the samples was then recorded at 517 nm and the ability of AgNPs to scavenge the DPPH radical was determined as follows (Eq. (1)):

$$\text{DPPH scavenging activity (\%)} = \frac{A_{\text{Control}} - A_{\text{Sample}}}{A_{\text{Control}}} \times 100 \quad (1)$$

2.4.2. Reducing power assay

The reducing properties of AgNPs were determined by standard method described elsewhere where Fe^{3+} ions reduced to Fe^{2+} ions [22]. Varying concentration of AgNPs solution (12.25, 25, 50, 100, and 200 µg/mL) was mixed with equal volumes of 0.2 M PBS (pH 6.6) and 1% $\text{K}_3\text{Fe}(\text{CN})_6$ (w/v) and incubated then in water bath shaker at 50 °C for 20 min. The reaction was terminated by adding 1% of TCA and the supernatant was collected by centrifugation at 15,000 rpm for 10 min. Further, 0.1% of FeCl_3 solution was added to the supernatant and the absorbance was finally measured at 700 nm.

2.5. Antibacterial assay

Antibacterial activity of Wedelia leaf extract mediated AgNPs was investigated against two different clinically isolated test pathogens *Escherichia coli* (Gram-negative) and *Listeria monocytogenes* (Gram-positive) by standard well-diffusion method [23]. Fresh overnight culture of each strain (100 µL) was swabbed uniformly onto the nutrient agar plates using sterile cotton swabs. A diameter of 10 mm of five circular wells was made using a sterilized gel puncture. 50 µL of leaf extract as control and varying concentration of AgNPs (12.25, 25, 50, 100, and 200 µg/mL) were then loaded serially into the well and incubated at room temperature for overnight. After 24 h, zone of inhibition (mm) was observed and mean of triplicates was tabulated.

2.6. In vitro cell viability assay

Hep G2 cell lines were purchased from NCCS, Pune. Standard MTT (yellow color tetrazole) assay was performed to study the viability of Hep G2 cell lines [24]. The assay relies on the mitochondrial activity of the viable cells by reducing the tetrazolium salt (MTT) to water-insoluble blue formazan product. Briefly, 1×10^5 cells/mL seeded into 96-well titre plates containing 100 µL of 5% FBS–DMEM were incubated in a 5% CO_2 incubator at 37 °C for 48 h and then exposed to varying concentrations of AgNPs (6.12, 12.25, 25, 50, 100 and 200 µg/mL) for 24 h under same experimental condition. After the exposure, the spent medium was changed and the cells were washed with cold PBS to remove the dead cells. 100 µL MTT (5 mg/mL) solution was added into each well and incubated in 5% CO_2 incubator for another 5 h. 100 µL DMSO was then added into each well after the incubation and aspirated to break the cells to dissolve the formazan crystals. The color developed was read spectrophotometrically at 570 nm. OD value was subjected to determine the cell viability (%) and IC_{50} values using following equation (Eq. (2)):

$$\text{Cell viability (\%)} = \frac{\text{Mean OD value of sample (AgNPs treated)}}{\text{Mean OD value of control (untreated)}} \times 100 \quad (2)$$

Further in vitro cell cytotoxicity or anticancer activity was determined using the following equation (Eq. (3)):

$$\text{Cell cytotoxicity or anticancer activity (\%)} = 100 - \text{cell viability (\%)} \quad (3)$$

2.7. LDH release assay

Lactate dehydrogenase (LDH) is an intracellular enzyme which specifically converts lactate to pyruvate. But when cell membrane loses its integrity, LDH releases into the extracellular medium and consequently increases the concentration of LDH which is proportional to the damaged cells. LDH release assay was performed using LDH assay kit. Briefly, the Hep G2 cells were pretreated with different concentrations of AgNPs (6.12, 12.25, 25, 50, 100 and 200 µg/mL) for 24 h, and 100 µL of cell free supernatant was then transferred into 96 well titre plates. 100 µL of substrate mixture from the kit containing catalyst diaphorase, NAD^+ and dye solution (iodonitrotetrazolium chloride and sodium lactate) was added into each well and incubated for additional 25 min at 37 °C. The OD_{440} was then measured which was directly proportional to LDH activity and concentration of AgNPs. The level of LDH released in culture media was expressed as LDH activity (IU/L).

3. Results and discussion

Wedelia chinensis is well known for its diverse pharmacological activities as it contains various bioactive molecules. In the present study, we investigated bioreduction properties of the plant extract to reduce silver ions to produce silver nanoparticles. To synthesize AgNPs, different volume (0.1–1.0 mL) of Wedelia leaf extract were mixed with aqueous AgNO_3 solution at 60 °C. A yellowish brown color appeared in the reaction tubes indicates the formation of AgNPs (Fig. 1a). Fig. 1b shows, surface plasmon resonance (SPR) band of the AgNPs are became broaden and concomitantly undergoes a red shift i.e. shifting the SPR bands towards higher wave length region as the concentration of leaf extract increase, suggesting a possible formation of larger particle due to aggregation [25]. Similarly red shift phenomenon of the AgNPs was previously reported by Link et al. According to their report such phenomenon was observed due to interaction between the surface capping molecules and the secondary reduction process on the surface of preformed nuclei [26]. However in the control experiment, without leaf extract no peak was observed. Further on mixing 1.0 mL Wedelia leaf extract with 9.0 mL of AgNO_3 solution under the same reaction condition, a well-defined peak was noticed, which increases as the reaction times increased (Fig. 1c). The strong absorption peak located at 408 nm confirms the reduction of silver ions to form the

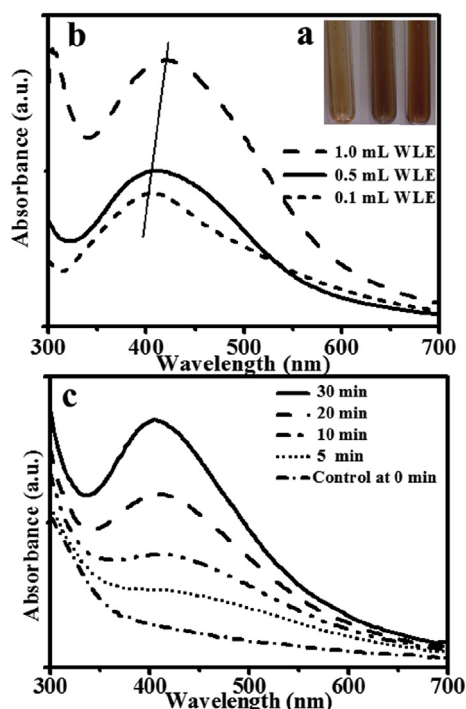


Fig. 1 – (a) Color changes after addition of different concentration of plant extract (1–10% v/v), (b) corresponding SPR spectra of AgNPs, and (c) time dependent absorption spectra of AgNPs.

metallic silver nanoparticles (AgNPs). The plausible mechanism of synthesis is proposed in Fig. 2. According to the scheme, monovalent silver ions and free radicals present in the polyphenolic compound in flavonoids, wedelolactones can form an intermediate metal-chelate complex which in turn undergoes oxidation of hydroxyl groups (–OH) present in the polyphenols of Wedelia leaf extract to carbonyl groups (C=O) and subsequent reduction of monovalent silver ions to zero-valent AgNPs. It is reported that antioxidant activity of polyphenol mainly resides on their ability to direct scavenge the molecular species of active oxygen and to donate the electrons or hydrogen atoms [27,28]. The TEM analysis was performed to visualize the size and shape of AgNPs formed. TEM micrograph shows the particles were predominantly spherical within 18–68.76 nm and distributed with little aggregation in solution (Fig. 3a and b). The distribution of AgNPs observed in the images could be due to the surface capping hence stabilizing effect of leaf extract over the AgNPs.

EDX, XRD, and XPS were used to characterize the biogenic AgNPs. EDX spectrum shows a strong signal at 3 keV confirmed the presence of silver atoms along with weak signals of oxygen and carbon (Fig. 4a). The weak signals might have generated from the biomolecules present on the surface of AgNPs and thus stabilizing the AgNPs upto 4 months after synthesis [29]. There is also a strong signal for aluminum (Al) which has

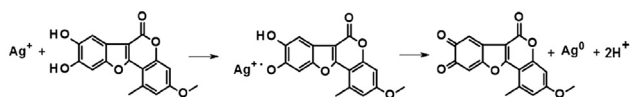


Fig. 2 – Plausible mechanism of biosynthesis of AgNPs.

originated from Al SEM grid used for sample analysis. XRD pattern of AgNPs shows clear peaks at 38.08° , 44.26° , 64.67° , and 77.54° (Fig. 4b) correspond to miller indices of (1 1 1), (2 0 0), (2 2 0), and (3 1 1) of zero-valent silver, respectively [30]. The lattice constant $a = 4.086 \text{ \AA}$ calculated from the XRD spectrum was good agreement with standard diffraction data JCPDF Card No. 03-0921. The average diameter of particle (D) was estimated to be 31.68 nm (Table 1) using Scherrer's equation $D = K\lambda/\beta_s \cos\theta$, where λ is X-ray wavelength (1.5406 Å), K is the shape dependent Scherrer's constant (0.94), θ is the Bragg angle, and β_s is X-ray line width (FWHM). Wide base corresponding to the peak indirectly indicates the presence small particle where little changes in the peak positions confirms the presence of bio-molecules on the crystal [31,32]. The XRD analysis strongly supports the evidence of formation of bioreduced silver nanocrystals obtained from UV–vis spectra and TEM images. Further, to study the chemical state of the AgNPs, XPS analysis was carried out. Deconvoluted spectra in the Ag 3d region show binding energies of 367.90 and 373.99 eV due to Ag $3d_{5/2}$ and Ag $3d_{3/2}$ respectively corresponding to Ag (0) state (Fig. 4c).

FTIR measurements were carried out to identify the possible biomolecules present in aqueous Wedelia leaf extract responsible for the bioreduction and stabilization of silver nanocrystals. The spectra of leaf extract were recorded and compared before and after addition of silver nitrate (Fig. 5). The interferogram of dried leaf extract before the reaction shows prominent peak at 1022, 1326, 1696, 2929, 3409 cm^{-1} represent the complex nature of the biomolecules (Fig. 5a). The very strong absorption bands centered at around 1022, 1326, 1696 cm^{-1} may arise from C–O, C–O–C and C=O stretching modes of vibration, respectively [33,34]. A moderate intense peak located at around 2929 cm^{-1} is probably due to presence of C–H deformation vibration [32]. Additionally, a broad band centred at 3409 cm^{-1} was observed confirming the O–H stretching vibrations, present in the leaf extract [35]. Most of the characteristic vibrational bands, are originated from the water soluble compounds like polyphenols, flavonoids, triterpenoids, wedelolactones etc. present in the Wedelia leaf extract. The FTIR spectrum of biosynthesized AgNPs exhibited few distinct peaks in the range of 1080, 1421, 1626, 2940 and 3463 cm^{-1} (Fig. 5b). Further, comparison study between the FTIR spectrum of leaf extract and biosynthesized AgNPs showed only minor changes in the position of absorption bands. On the basis of IR data, it may be inferred that the biomolecules present in WLE significant have bio-reduction property to synthesize AgNPs.

DPPH assay was carried out to measure the efficiency of antioxidants to scavenge the free radical from DPPH. The reduction of DPPH was assessed spectrophotometrically by observing the decrease in absorbance due to the formation of stable DPPH-H molecule (reduced form) [36]. Fig. 6a shows the free radical scavenging activity of AgNPs increased gradually with increasing concentration of AgNPs (12.25–200 $\mu\text{g/mL}$). The maximum scavenging activity of AgNPs (200 $\mu\text{g/mL}$) was found to be $80.2 \pm 0.15\%$ as compared to control leaf extract ($67.53 \pm 0.34\%$), and reference L-ascorbic acid ($96.32 \pm 0.33\%$). Similar antioxidant activity of the AgNPs was previously reported by Chanthini et al. [37]. Further, the reducing power of Wedelia leaf extract, AgNPs, and AA was determined based on reduction of Fe^{3+} ions to Fe^{2+} ions. As shown in Fig. 6b, the

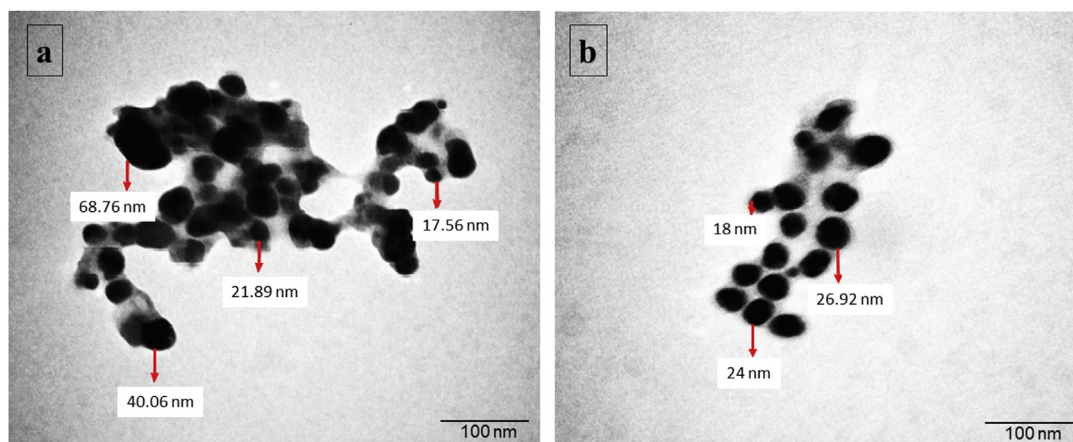


Fig. 3 – (a and b) TEM micrographs of biosynthesized spherical shaped AgNPs.

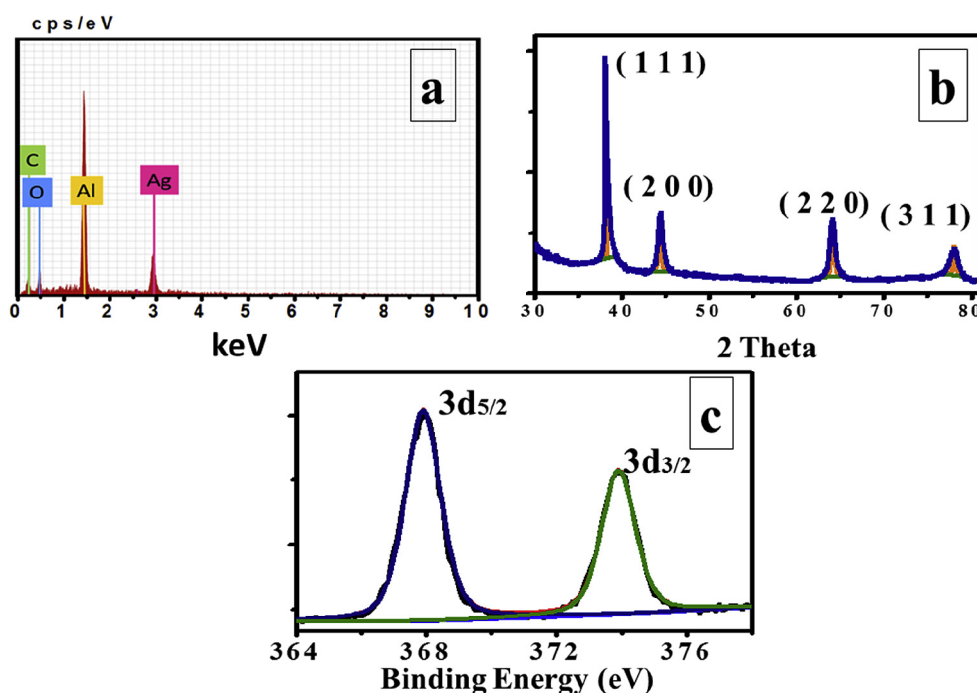


Fig. 4 – (a) EDX, (b) XRD, and (c) XPS spectra of AgNPs synthesized using WLE.

reducing capacity of the biogenic AgNPs (200 $\mu\text{g/mL}$) was observed higher (absorbance 0.81 ± 0.146) compared to control leaf extract (absorbance 0.18 ± 0.006) and lower than the reference L-ascorbic acid (0.86 ± 0.048). Because of their free radical scavenging properties, AgNPs can be consider as a potential candidate in the management of cancer, diabetes, AIDS, neurodegenerative disease etc.

Table 1 – Particle size of biosynthesized AgNPs.

2 θ (Ref.)	2 θ (Exp.)	FWHM (Exp.)	Miller indices	Particle size	Average size (nm)
38.09	38.08	0.3408	111	27.17	31.68
44.59	44.26	0.3346	200	26.77	
64.67	64.06	0.3346	220	29.25	
77.54	77.93	0.2448	311	43.56	

Biosynthesized AgNPs showed significant antimicrobial activity against both the pathogenic bacteria i.e. *E. coli* and *L. monocytogenes* (Fig. 7a and b). Mean diameter of the inhibitory zone (mm) around each well was measured and tabulated in Table 2. Result shows Wedelia leaf extract didn't exhibit any significant antibacterial activity against test pathogens even at high concentration, might be due to the active constituents responsible for antibacterial activity is not present in aqueous leaf extract. It was also observed that maximum zone of inhibition increases with increasing concentration of AgNPs where *E. coli* (Gram-negative) exhibited higher zone of inhibition as compared to *L. monocytogenes* (Gram-positive) (Fig. 7c). This might be due to the presence of rigid peptidoglycan layer on Gram-positive bacterial cell wall as compared to Gram-negative bacteria preventing the AgNPs to penetrate, resulting lower zone of inhibition. The exact mechanism

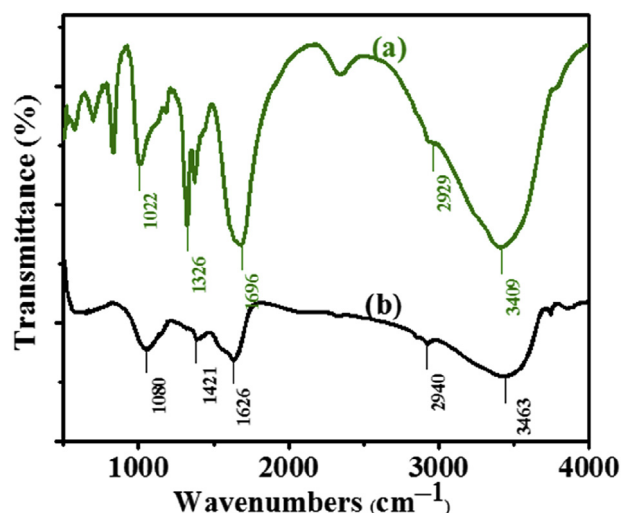


Fig. 5 – FTIR spectrum of (a) WLE (alone) and (b) synthesized AgNPs from WLE.

behind the antibacterial activity of AgNPs was not very clear, but many proposals are put forward for the same. Most accepted hypothesis are i) formation of pits on the outer membrane progressively release the lipopolysaccharides and membrane proteins [38], ii) cells treated with AgNPs lead to increase the conductivity resulting leakage of the intracellular molecules [39] and, iii) AgNPs interrupts the ATP metabolism and DNA replication preferentially by targeting the sulfur and phosphorous rich macromolecules resulting programmed cell death [40].

The cytotoxic response of various concentrations of bio-synthesized AgNPs (6.12–200 $\mu\text{g/mL}$) was determined against transformed Hep G2 cell lines by MTT and LDH assays. Cell lines without AgNPs were considered as control. Experimental analysis of the sample showed a dose-dependent cytotoxicity; where cell viability decreased with increasing concentration of AgNPs (Fig. 8a–c). At concentration of 6.12 $\mu\text{g/mL}$, AgNPs was able to inhibit the cell lines's growth by less than 11.77% whereas at 200 $\mu\text{g/mL}$ concentration, showed significant in vitro cytotoxic effect (>93.34% cell death) after 24 h of incubation. Reduction of cell viability by ~50% in comparison

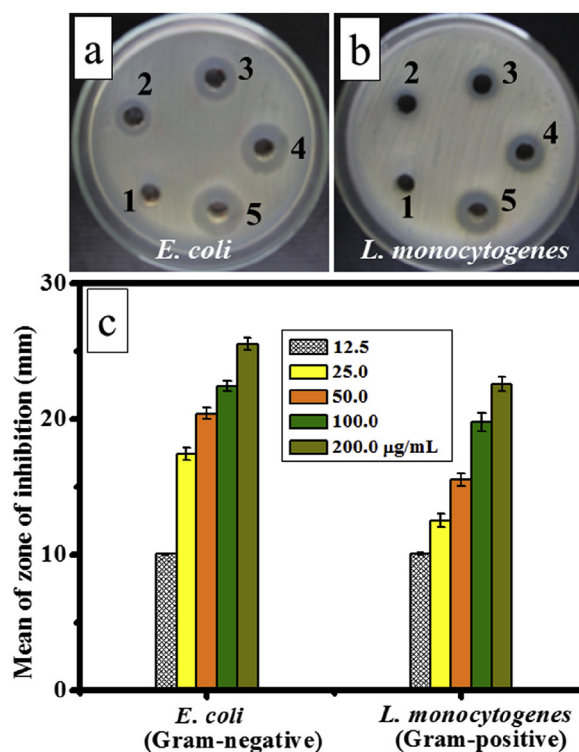


Fig. 7 – Antibacterial activity (a) on Gram-negative bacteria (*E. coli*), (b) on Gram-positive bacteria (*L. monocytogenes*), and (c) mean zone of inhibition (mm) of biogenic AgNPs synthesized against pathogenic bacterial strains.

with the control was achieved at a dose of 25 $\mu\text{g/mL}$ (IC_{50}) concentration of AgNPs (Fig. 8d). The chi-square values were significant at $p < 0.05$ level. This data strongly suggests that the AgNPs may possess anticancer/antiproliferative properties. The cytotoxic response of the AgNPs was further validated by measuring LDH leakage from the treated cells. LDH is considered as a cytoplasmic or intracellular stable biomarker for the viable cells, thereby presence of LDH into the cell free medium demonstrates the membrane disruption or cell injury, resulting cell death [41]. As expected, AgNPs caused cytotoxicity in a dose-dependent manner and subsequently

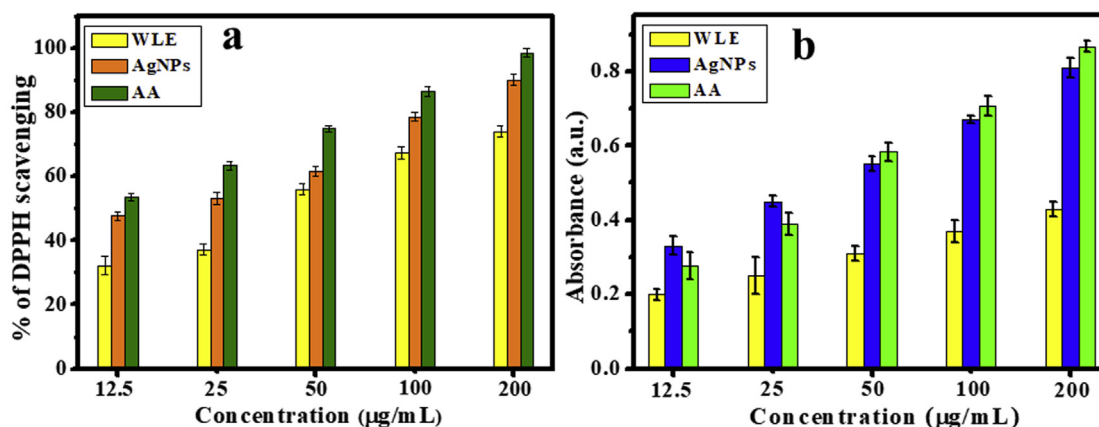


Fig. 6 – (a) DPPH free radical scavenging activity, and (b) Reducing power of WLE, biosynthesized AgNPs, and AA (L-ascorbic acid) at different concentrations (12.5–200 $\mu\text{g/mL}$).

Table 2 – Antibacterial activity of biosynthesized AgNPs against test bacterial pathogens.

Test		Zone of inhibition (mm)						
Conc.	bacteria	WLE	AgNPs					Amp.
(µg/mL) ^a		100	12.25	25	50	100	200	20
	<i>E. coli</i>	NI	NI	17.2±0.47	20.5±0.19	22.4±0.46	25.4±0.83	35.1±0.43
	<i>L. monocytogenes</i>	NI	NI	11.9±0.39	14.9±0.84	19.1±0.90	21.7±0.17	27.3±0.21

^aA stock solution of 1 mg/mL was prepared.

NI : No inhibition

Data expressed as means of triplicate \pm standard deviation.

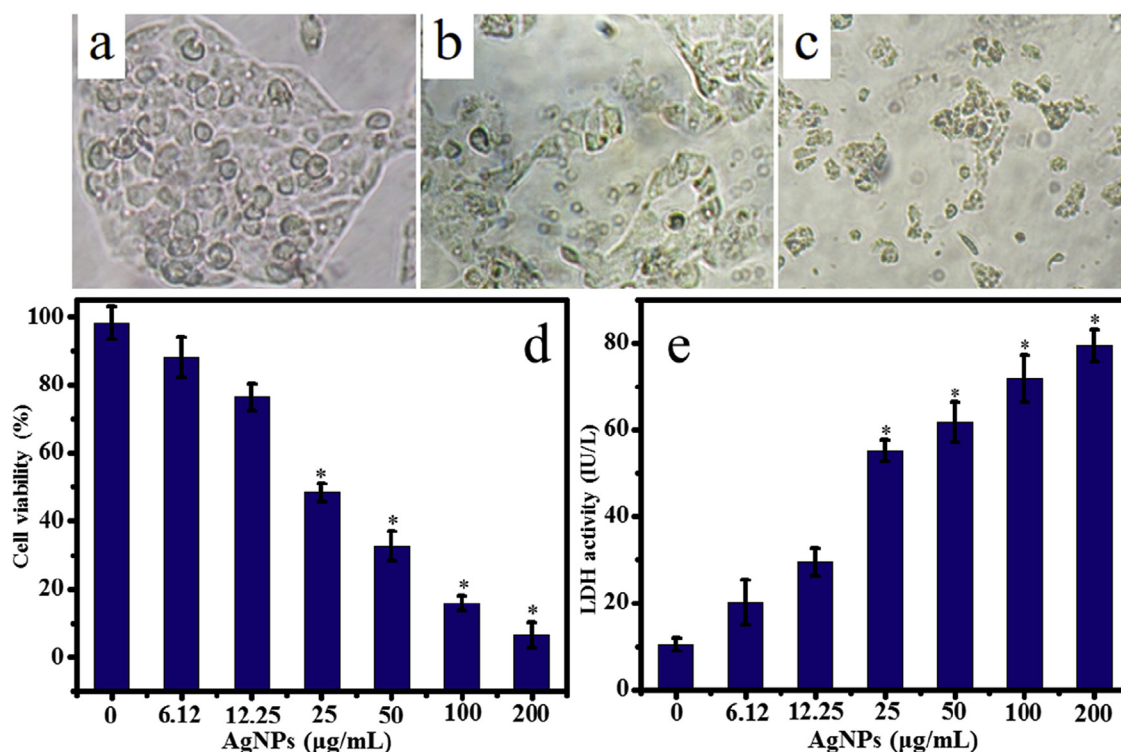


Fig. 8 – Inverted microscopic images of Hep G2 cell lines (10 \times magnification) after 24 h incubation (a) control cell lines, (b) AgNPs treated cell lines at IC₅₀, (c) AgNPs (200 $\mu\text{g/mL}$) treated cell lines, (d) effects of AgNPs on the viability of Hep G2 cell lines, and (e) effect of AgNPs on LDH activity on Hep G2 cell lines. (*) indicates a statistically significant difference compared to control ($p < 0.05$).

increase in LDH leakage, as compared to control cells. The Hep G2 cells treated with 200 $\mu\text{g/mL}$ of AgNPs showed the highest LDH activity in the cell culture supernatant, which is indicative of maximum cellular damage and toxicity (Fig. 8e). The cytotoxicity was observed due to the generation of reactive

oxygen species (ROS) like hydroxyl radical, hydrogen peroxide, superoxide radical, singlet oxygen, etc. These radical induces damage to various cellular macromolecules like DNA, lipids, proteins and subsequently leading to cell death by apoptosis or necrosis [42,43]. This result suggested

that the leaf mediated synthesized silver nanoparticles possess great sensitivity to cancer cells and can display potential applications in cancer chemoprevention and chemotherapy.

4. Conclusion

Photosynthesis of spherical nanosilver particles was effectively established without using any templates, additives or accelerants. Flavonoid/wedelolactone comprises functional groups as evident from the FTIR analysis might have associated in the reduction and stabilization of biogenic AgNPs. Synthesized AgNPs possess significant antioxidant, and antibacterial activity as compared to the control one. The nanoparticles also showed an IC_{50} value of 25 $\mu\text{g/mL}$ against hepatocellular carcinoma Hep G2 cell lines. Thus it can be concluded that Wedelia leaf extract mediated AgNPs synthesis can be considered as a cheap and ecofriendly approach, possessing various biomedical applications. Further, in-depth study on antioxidant, antibacterial and anticancer property in mammalian immune system and mechanism behind the action is essential for clinical significance.

Acknowledgements

The authors convey their hearty thanks to Department of Industrial Biotechnology, Bharath University for providing laboratory facilities and Department of Nanotechnology, SRM University for supporting EDX, FTIR, and XRD analysis.

REFERENCES

- [1] Bar H, Bhui DK, Sahoo GP, Sarkar P, De SP, Misra A. Green synthesis of silver nanoparticles using latex of *Jatropha curcas*. *Colloids Surf A* 2009;339:134–9.
- [2] Veluswamy P, Suhasini S, Khan F, Ghosh A, Abhijit M, Hayakawa Y, et al. Incorporation of ZnO and their composite nanostructured material into a cotton fabric platform for wearable device applications. *Carbohydr Polym* 2017;157:1801–8.
- [3] Shah AH, Manikandan E, Ahamed MB, Mir DA, Mir SA. Antibacterial and blue shift investigations in sol–gel synthesized $\text{Cr}_x\text{Zn}_{1-x}\text{O}$ nanostructures. *J Lumin* 2014;145:944–50.
- [4] Foldbjerg R, Dang DA, Autrup H. Cytotoxicity and genotoxicity of silver nanoparticles in the human lung cancer cell line, A549. *Arch Toxicol* 2011;85:743–50.
- [5] Borm PJA, Kreyling W. Toxicological hazards of inhaled nanoparticles potential implications for drug delivery. *J Nanosci Nanotechnol* 2004;4:521–31.
- [6] Sukirtha R, Priyanka KM, Antony JJ, Kamalakannan S, Thangam R, Gunasekaran P, et al. Cytotoxic effect of green synthesized silver nanoparticles using *Melia azedarach* against *in vitro* HeLa cell lines and lymphoma mice model. *Process Biochem* 2012;47:273–9.
- [7] Hussain SM, Javorina AK, Schrand AM, Duhart HM, Ali SF, Schlager JJ. The interaction of manganese nanoparticles with PC-12 cells induces dopamine depletion. *Toxicol Sci* 2006;92:456–63.
- [8] Stolle LB, Hussain S, Schlager JJ, Hofmann MC. *In vitro* cytotoxicity of nanoparticles in mammalian germline stem cells. *Toxicol Sci* 2005;88:412–9.
- [9] Chopra I. The increasing use of silver-based products as antimicrobial agents: a useful development or a cause for concern? *J Antimicrob Chemother* 2007;59:587–90.
- [10] Sen S, Chakraborty R, Sridhar C, Reddy Y, De B. Free radicals, antioxidants, diseases and phytomedicines, current status and future prospect. *Int J Pharm Sci Rev Res* 2010;3:91–100.
- [11] Wu D, Cederbaum AI. Alcohol, oxidative stress, and free radical damage. *Alcohol Res Health* 2003;27:277–84.
- [12] Soares JR, Dins TCP, Cunha AP, Almeida LM. Antioxidant activity of some extracts of *Thymus zygis*. *Free Radic Res* 1997;26:469–78.
- [13] Kanipandian N, Kannan S, Ramesh R, Subramanian P, Thirumurugan R. Characterization, antioxidant and cytotoxicity evaluation of green synthesized silver nanoparticles using *Cleistanthus collinus* extract as surface modifier. *Mater Res Bull* 2014;49:494–502.
- [14] Hart AE, Akers DB, Gorosh S, Kitchens CL. Reverse micelle synthesis of silver nanoparticles in gas expanded liquids. *J Supercrit Fluids* 2013;79:236–43.
- [15] Tripathy A, Raichur AM, Chandrasekaran N, Prathna TC, Mukherjee A. Process variables in biomimetic synthesis of silver nanoparticles by aqueous extract of *Azadirachta indica* (Neem) leaves. *J Nanopart Res* 2010;12:237–46.
- [16] Zhang Y, Chang G, Liu S, Lu W, Tian J, Sun X. A new preparation of Au nanoplates and their application for glucose sensing. *Biosens Bioelectron* 2011;28:344–8.
- [17] Gardea-Torresdey JL, Parsons JG, Dokken K, Peralta-Videa JR, Troiani H, Santiago P, et al. Formation and growth of Au nanoparticles inside live alfalfa plants. *Nano Lett* 2002;2:397–401.
- [18] Shankar SS, Ahmad A, Sastry M. Geranium leaf assisted biosynthesis of silver nanoparticles. *Biotechnol Prog* 2003;19:1627–31.
- [19] Shankar SS, Rai A, Ankamwar B, Singh A, Ahmad A, Sastry M. Biological synthesis of triangular gold nanoprisms. *Nat Mater* 2004;3:482–8.
- [20] Koul S, Pandurangan A, Khosa RL. *Wedelia chinensis* (Asteraceae) – an overview. *Asian Pac J Trop Biomed* 2012;2:1169–75.
- [21] Choi CW, Kim SC, Hwang SS, Choi BK, Ahn HJ, Lee MY, et al. Antioxidant activity and free radical scavenging capacity between Korean medicinal plants and flavonoids by assay guided comparison. *Plant Sci* 2002;163:1161–8.
- [22] Oyaizu M. Studies on product of browning reaction prepared from glucose amine. *Jpn J Nutr* 1986;44:307–15.
- [23] Dipankar C, Murugan S. The green synthesis, characterization and evaluation of the biological activities of silver nanoparticles synthesized from *Iresine herbstii* leaf aqueous extracts. *Colloids Surf B* 2012;98:112–9.
- [24] Mosmann T. Rapid colorimetric assay for cellular growth and survival: application to proliferation and cytotoxicity assays. *J Immunol Methods* 1983;65:55–63.
- [25] Kannan N, Mukunthan KS, Balaji S. A comparative study of morphology, reactivity and stability of synthesized silver nanoparticles using *Bacillus subtilis* and *Catharanthus roseus* (L.) G. Don. *Colloids Surf B* 2011;86:378–83.
- [26] Link S, El-Sayed MA. Spectral properties and relaxation dynamics of surface plasmon electronic oscillations in gold and silver nanodots and nanorods. *J Phys Chem B* 1999;103:8410–26.
- [27] Saxena A, Tripathi RM, Zafar F, Singh P. Green synthesis of silver nanoparticles using aqueous solution of *Ficus benghalensis* leaf extract and characterization of their antibacterial activity. *Mater Lett* 2012;67:91–4.
- [28] Moran JF, Klucas RV, Grayer RJ, Abian J, Becana M. Complexes of iron with organic compounds from soybean nodules and

- other legume tissues: prooxidant and antioxidant properties. *Free Radic Biol Med* 1997;22:861–70.
- [29] Ahmad A, Senapati S, Islam Khan M, Kumar R, Ramani R, Srinivas V, et al. Intracellular synthesis of gold nanoparticles by a novel alkalotolerant actinomycete, *Rhodococcus* species. *Nanotechnology* 2003;14:824–8.
- [30] Khalilzadeh MA, Borzoo M. Green synthesis of silver nanoparticles using onion extract and their application for the preparation of a modified electrode for determination of ascorbic acid. *J Food Drug Anal* 2016;24:796–803.
- [31] Binupriya AR, Sathishkumar M, Yun SI. Myco-crystallization of silver ions to nanosized particles by live and dead cell filtrates of *Aspergillus oryzae* var. *viridis* and its bactericidal activity toward *Staphylococcus aureus* KCCM 12256. *Ind Eng Chem Res* 2010;49:852–8.
- [32] Sathishkumar M, Sneha K, Won SW, Cho CW, Kim S, Yun YS. *Cinnamon zeylanicum* bark extract and powder mediated green synthesis of nano-crystalline silver particles and its bactericidal activity. *Colloids Surf B* 2009;73:332–8.
- [33] Philip D. *Mangifera indica* leaf-assisted biosynthesis of well-dispersed silver nanoparticles. *Spectrochim Acta Part A* 2011;78:327–31.
- [34] Dubey SP, Lahtinen M, Sillanpää M. Green synthesis and characterizations of silver and gold nanoparticles using leaf extract of *Rosa rugosa*. *Colloids Surf A* 2010;364:34–41.
- [35] Shah AH, Manikandan E, Ahmed MB, Ganesan V. Enhanced bioactivity of Ag/ZnO nanorods-A comparative antibacterial study. *J Nanomed Nanotechnol* 2013;4:1000168–73.
- [36] Schlesier K, Harwat M, Bohm V, Bitsch R. Assessment of antioxidant activity by using different in vitro methods. *Free Radic Res* 2002;36:177–87.
- [37] Chanthini AB, Balasubramani G, Ramkumar R, Sowmiya R, Balakumaran MD, Kalaichelvan PT. Structural characterization, antioxidant and in vitro cytotoxic properties of seagrass, *Cymodocea serrulata* (R.Br.) Asch. & Magnus mediated silver nanoparticles. *J Photochem Photobiol B* 2015;153:145–52.
- [38] Amro NA, Kotra LP, Wadu-Mesthrige K, Bulychev A, Mobashery S, Liu G. High-resolution atomic force microscopy studies of the *Escherichia coli* outer membrane: structural basis for permeability. *Langmuir* 2000;16:2789–96.
- [39] Krishnaraj C, Jagan EG, Rajasekar S, Selvakumar P, Kalaichelvan PT, Mohan N. Synthesis of silver nanoparticles using *Acalypha indica* leaf extracts and its antibacterial activity against water borne pathogens. *Colloids Surf B* 2010;76:50–6.
- [40] Chitra K, Manikandan A, Antony SA. Effect of poloxamer on *Zingiber officinale* extracted green synthesis and antibacterial studies of silver nanoparticles. *J Nanosci Nanotechnol* 2016;16:758–64.
- [41] Mitchell DB, Santone KS, Acosta D. Evaluation of cytotoxicity in cultured cells by enzyme leakage. *J Tissue Cult Meth* 1980;6:113–6.
- [42] Venugopal K, Rather HA, Rajagopal K, Shanthi MP, Sheriff K, Illiyas M, et al. Synthesis of silver nanoparticles (AgNPs) for anticancer activities (MCF 7 breast and A549 lung cell lines) of the crude extract of *Syzygium aromaticum*. *J Photochem Photobiol B* 2016;167:282–9.
- [43] Venugopal K, Ahmad H, Manikandan E, Arul KT, Kavitha K, Moodley MK, et al. The impact of anticancer activity upon *Beta vulgaris* extract mediated biosynthesized silver nanoparticles (Ag–NPs) against human breast (MCF-7), lung (A549) and pharynx (Hep-2) cancer cell lines. *J Photochem Photobiol B* 2017;173:99–107.